Correlation of seismic attributes and geo-mechanical properties to the rate of penetration in the Mississippian Limestone, Oklahoma

Xuan Qi, Joseph Snyder, Tao Zhao, Kurt J. Marfurt, and Matthew J. Pranter[1]

ConocoPhillips school of Geology and Geophysics, University of Oklahoma, USA

100 E. Boyd St., Norman, Oklahoma, 73019

sherryqixuan@ou.edu

Joseph.C.Snyder-1@ou.edu

tao-zhao@ou.edu

kmarfurt@ou.edu

matthew.pranter@ou.edu,

Acknowledgement

We thank the sponsors of the "Mississippi Lime" and Attribute Assisted Seismic Processing & Interpretation (AASPI) Consortia at the University of Oklahoma: Anadarko, Arcis, BGP, BHP Billiton, Lumina Geophysical, Chesapeake Energy, Chevron, ConocoPhillips, Devon Energy, EnerVest, ExxonMobil, Geophysical Insights, Institute of Petroleum, Marathon Oil, Newfield Exploration, Occidental Petroleum, Petrobras, Pioneer Natural Resources, QEP, Remark Energy Technology, Schlumberger, Shell, SM Energy, Southwestern Energy, and Tiptop Energy (Sinopec). We especially thank Chesapeake Energy for providing the 3D seismic and well data. Petrel 2015 software was graciously provided by Schlumberger. Seismic attributes and the proximal Support Vector Machine (PSVM) results were generated using AASPI software. We would like to acknowledge CGG GeoSoftware for its donation of its software Hampson Russell, that was used for seismic inversion analysis and porosity estimation. We would like to thank our colleague Mr. Abdulmohsen AlAli for generating seismic pre-stack inversion.

Abstract

The rate of penetration (ROP) measures drilling speed, which is indicative of the overall time and in general, the cost of the drilling operation process. ROP depends on many engineering factors; however, if these parameters are held constant, ROP is a function of the geology. We examine ROP in the relatively heterogeneous Mississippian Limestone reservoir of north-central Oklahoma where hydrocarbon exploration and development have been present in this area for over fifty years. A 400 mi^2 (1036 km^2) 3D seismic survey and 51 horizontal wells were used to compute seismic attributes and geo-mechanical properties in the area of interest. Previous Tunnel Boring Machines (TBM) studies have shown that ROP can be correlated to rock brittleness and natural fractures. We therefore hypothesize that both structural attributes and rock properties should be correlated to ROP in drilling horizontal wells. We use a proximal support vector machine (PSVM) to link rate of penetration to seismic attributes and mechanical rock properties with the objective to better predict the time and cost of the drilling operation process. Our workflow includes three steps: exploratory data analysis, model validation, and classification. Exploratory data analysis using 14 wells indicate high ROP is correlated with low porosity, high lambda-rho, high mu-rho, low curvedness, and high P-impedance. Low ROP was exhibited by wells with high porosity, low lambda-rho, low mu-rho, high curvedness and low P-impedance. Validation of the PSVM model using the remaining 37 wells gives an $R^2 = 0.94$. Using these five attributes and 14 training wells, we used PSVM to compute a ROP volume in the target formation. We anticipate that this process can help better predict a budget or even reduce the cost of drilling when an ROP assessment is made in conjunction with reservoir quality and characteristics.

Introduction

Drilling and completion of horizontal wells are the largest expenses in unconventional reservoir plays, where the cost of drilling a well is proportional to the time it takes to reach the target objective. Accordingly, the faster the desired penetration depth and offset is achieved, the lower the cost of the drilling process. The rate of penetration (ROP) is measured in all wells, but rarely examined by geoscientists. ROP depends on many factors, but the primary factors are weight on the drill bit, drill bit rotation speed, drilling fluid-flow rate, and the characteristics of the formation being drilled (Bourgoyne et al., 1986). In this study, all wells were drilled within a two-year period using similar drilling parameters, allowing investigation of the formation characteristics on the ROP.

Various approaches have been applied to estimate ROP. One of the main challenges for ROP estimation is the variability in the interplay between the rock and drilling speed (Farrokh et al., 2012). A "drill-off test" is a method primarily used to determine an optimum ROP for a set of conditions; however, a limitation of the drill-off test is that this process produces a static weight only valid for limited conditions during the test. The drill-off test does not work well under more complex geological conditions (King and Pinckard, 2000). Gong and Zhao (2007) utilized numerical simulations to investigate how rock properties affected penetration rates in Tunnel Boring Machines (TBM) and found that an increase in rock brittleness caused an increase in penetration rate. Later, a numerical model was created to model penetration rate for TBM's by Gong and Zhao (2009), who found that an increase in compression strength decreased ROP and an increase in volumetric joint count increased ROP.

In addition to well logs and cores, seismic attributes are widely used to predict lithological and petrophysical properties of reservoirs. For example, curvature anomalies commonly indicate an increase in rock strain, which in turn can be used to infer fractures (White et al., 2012). Impedance inversion is currently the most direct seismic-based estimate of rock properties. Seismic-impedance inversion results have been used to predict fault zones, potential fractures, and lithology in the Mississippian Limestone (Dowdell et al., 2013; Roy et al., 2013; Verma et al., 2013; Lindzey et al., 2015;). Young's modulus, E, and Poisson's ratio, υ, calculated from bulk density, ρ, compressional velocity, V_p, and shear velocity, V_s logs can be used to estimate rock brittleness (Harris et al., 2011).

Drilling and borehole measurements such as ROP are usually not linearly related to volumetric seismic attributes, such that the use of multilinear regression is limited. Artificial-Neural Networks (ANN) is commonly used to link attributes to properties such as gamma-ray response (Verma et al., 2013), Total Organic Carbon (TOC) (Verma et al., 2016), and well production (Da Silva et al., 2012). The Proximal Support Vector Machine (PSVM) method is a more recent innovation that has been successfully used to predict brittleness (Zhang et al., 2015). PSVM utilizes pattern recognition and classifies points by mapping them to a higher dimension before assigning them to categories. PSVM has been applied in seismic facies recognition (e.g. channels, mass-transport complexes, etc.) (Zhao et al., 2015) and lithofacies classification (Zhao et al., 2014). Zhao et al. (2014) used PSVM to categorize shale and limestone on well logs with training inputs of gamma-ray and sonic logs.

With the recent onset of unconventional techniques such as horizontal drilling and hydraulic fracturing, the Mississippian Limestone has seen a growth in activities. Where operators once targeted structural traps with vertical wells, now they target stratigraphic traps with horizontal wells (Lindzey et al., 2015). Such horizontal wells require a better understanding of the variability within the Mississippian Limestone in order to increase the success and efficiency of precisely targeted directional wells. Throughout this study, a workflow is presented to establish a relationship between seismic attributes and rock mechanical properties with ROP in order to optimize well placement and decrease the drilling cost.

Geological Setting

The Mississippian Limestone is a broad informal term that refers to dominantly carbonate deposits of the Mid-continent (Parham and Northcutt., 1993). The main depositional environment represented in north-central Oklahoma is associated with the east-west trending ramp margin of the Burlington shelf of a starved basin environment (Costello et al., 2013). The thickness of the Mississippian Limestone ranges from 350 ft (106.7 m) to 700 ft (213.4 m) north to south over the study area (Costello et al., 2013).

Mississippian Limestone in the study area were deposited in a southward prograding system near the shelf margin during Osagean and Meramecian time (Costello et al., 2013). This environment has resulted in commonly acknowledged facies within the Mississippian carbonates, ranging from shale, chert conglomerate, tripolitic chert, dense chert, altered chert-rich limestone, dense limestone, to shale-rich limestone (Lindzey et al., 2015). In the study area, tripolitic chert is most prevalent in the Upper Mississippian zones and rapidly decreases in abundance at depth greater than 150 ft (45.7 m) below the pre-Pennsylvanian unconformity (Lindzey et al., 2015).

During the early Mississippian, warm oxygenated water covered much of the ramp in the study area. Sponge-microbe bioherms formed elongate mounds below storm wave base and produced abundant SiO2 spicules which led to formation of spicule-rich wackestones and packsontes (Lindzey et al., 2015). Limestone and cherty limestone rich in marine fauna were the dominant sediments deposited at this time (Parham and Northcutt., 1993).

Regional uplift occurred during the Pennsylvanian, creating the Pennsylvanian unconformity that overlies most of the Mississippian in the midcontinent (Parham and Northcutt, 1993). The uplift not only removed large sections of rock but also reworked and caused alteration at the top of the Mississippian section and created detrital deposits of reworked

Mississippian-aged rocks (Rogers, 2001). These altered sections of rocks are comprised of highly porous tripolitic chert and very dense glass-like chert. The leaching due to meteoric waters during relative sea-level fall has led to karstification and the formation of caverns and solution-channel features (Parham and Northcutt., 1993).

In the study area, diagenesis left intensely altered Mississippian Limestone after deposition, and one of the most prominent of these diagenetic features is silica replacement (Lindzey et al., 2015). Water washed through the pores and redistributed the siliceous volcanic ash and some macrofossils, which left extensive micro-scale porosity (Lindzey et al., 2015). The dissolved silica precipitated in pore space and partially or completely replaced some carbonate fossils (Lindzey et al., 2015). Pore Sediment structures are not well preserved due to the strong diagenetic overprint. Chert nodules are present, especially in highly reworked and bioturbated zones. Fractures are often filled with silica or calcite (Costello et al., 2013).

Molds, fractures, channels and especially vugs are the most prominent pore type observed in the Mississippian interval of the study area (Lindzey et al., 2015). Vuggy porosity is often associated with tripolite, but also exists in the other dominant facies. In many places where silica replacement took place, extensive secondary porosity formed in the shape of vugs (Rogers, 2001). Moldic porosity is also common, especially in packstone and grainstone facies that exhibit more skeletal grains. Moldic porosity develops by dissolution of sponge spicules (Montgomery et al., 1998). Fracture and channel porosity both exist but are less abundant compared to the other pore types (Lindzey et al., 2015).

Methodology

In 2010, Chesapeake Energy acquired a 400 mi^2 (1036 km^2) 3D seismic survey in Woods County, Oklahoma **(Figure 1a)**. The seismic processing workflow included refraction statics, velocity analysis, residual statics, prestack time migration, Frequency-Space-Time (FXY) predictive noise rejection, and Ormsby filtering. The overall data quality is excellent. The signal to noise ratio (S/N) is relatively high and the wavelet amplitude appears continuous throughout the Mississippian target. The data set includes digital well logs and mud logs for 83 wells, consisting of 52 horizontal and 31 vertical wells. For the ROP analysis, only horizontal wells were used. These data consisted of 52 gamma-ray logs, 51 mud logs, and 18 of them are open-hole logs.

The wells in the area of interest were drilled by the same operator in a similar time period; therefore we assume consistency between the wells regarding weight on bit, mud type, and bit type. This study evaluates the impact of geological properties on the ROP. The work flow contains three steps: training, validation, and classification **(Figure 2)**. Pre-stack inversion and seismic-attribute volumes were generated for the Mississippian Limestone and converted to depth. Geomechanical rock properties (from seismic inversion) and seismic-attribute values were interpolated and then extracted along each wellbore every 2 ft (0.61 m) corresponding to the well-coordinate system from the mud logs. The mud logs give ROP in units of min/ft, which is an inverse velocity. We define the inverse velocity to be the Cost of Penetration (COP). The mean and standard deviation of COP for the 51 horizontal wells resulted in two categories: high and low COP with average values of 27 and 2.5 min/ft (89 min/m and 8.2 min/m), respectively **(Figure 3)**. Each coordinate location is assigned a COP category and a set of values including seismic attributes and geomechanical rock properties. The category and values for 30% of the wells were used as inputs to train the model. The remaining 70% of the wells were used to validate the model. When an optimal accuracy is reached, the model is used to classify the entire data set where wells have yet to be drilled and no COP data are available.

Time-depth conversion

Formation tops for the Lansing, Mississippian and Woodford units were interpreted on the time-migrated seismic data in the time domain and on well logs in the depth domain. A conversion velocity model ($V_0(x, y)$) was built using commercial software PETREL (© Schlumberger), where velocity, V_0 is defined at the top of the Lansing datum, $Z_0(x, y)$. Depth, Z, is calculated by adding the depth below the Lansing, $\Delta Z = V_0(x, y) \times \left[t - t_0(x, y)\right]$ to the datum. The well tops were used as a correction factor in the creation of the velocity model. Well data were assigned more weights than the seismic data. We followed the recommended settings to build the velocity model, such that a moving-average method was used as an interpolation approach for creating the new depth surfaces and an inverse-distance-squared algorithm was used to compute the inverse distance during the interpolation processes. Because the seismic horizons honored the faults in the study area, the velocity model is computed taking faults into consideration.

Geometric attributes

Geometric attributes for this dataset were generated using software AASPI developed at the University of Oklahoma. The attributes generated included: most positive curvature, k_1, most negative curvature, k_2, curvedness, $\sqrt{k_1^2 + k_2^2}$, shape index, $s = \frac{2}{\pi} ATAN(\frac{k_2 + k_1}{k_2 - k_1})$, coherent energy, and coherence. These attributes were chosen because of their ability to delineate the structural complexity in the area of interest. The sampling interval of these attributes is the same as the original seismic data volume, 110 ft by 110 ft (33.5 m by 33.5 m). In order to match the mud log coordinate spacing, linear interpolation was used to generate values at 2 ft (0.61 m) intervals.

Geomechanical rock properties

Geomechanical rock properties were derived from pre-stack inversion results using commercial software Hampson Russell (© CGG GeoSoftware). Data preconditioning steps, prior to a pre-stack seismic inversion included phase shift, bandpass filtering (10-15-110-120 Hz), parabolic Radon transform, and trim statics.

Exploratory data analysis

Exploratory data analysis consisted of evaluation of two different families of volumetric attributes as input to PSVM classification: geometric attributes and geomechanical rock properties with the goal of determining which attributes are most sensitive to COP in the heterogeneous Mississippian Limestone.

Geometric attributes are used to aid in the interpretation of folds and faults. Based on the TBM observation by Gong and Zhao (2007), we hypothesize that COP is affected by faults and fractures. Therefore we examined the correlation of the structural attributes coherence, dip magnitude, curvature, and curvedness to our two well clusters **(Figure 6).** The attribute histograms indicate little to no separation for coherence and dip magnitude; however, curvature and curvedness exhibit measurable separation. **Figure 4d** indicates that low curvedness correlates to low COP.

TBM analysis by Gong and Zhao (2007) also suggested that mechanical properties play a significant role in the variation of COP. Using prestack seismic inversion we computed porosity, lambda-rho, $\lambda\rho$, mu-rho, $\mu\rho$, and P-impedance volumes to analyze the Mississippian Limestone **(Figure 5)**. The P-impedance measures the product of density and seismic P velocity. $\lambda\rho$ and $\mu\rho$ are used to estimate lithology and geomechanical behavior such as the brittleness index (Perez and Marfurt, 2013). **Figures 4b, 4c, and 4e** show the high degree of separation for these rock properties. Low COP is related to low porosity, high $\lambda\rho$, high $\mu\rho$, and high P-impedance values. Conversely, high porosity, low $\lambda\rho$, low $\mu\rho$, and low P-impedance values are indicative of high COP. These differences were used to train the PSVM model and classify COP data based on the geomechanical rock properties within the Mississippian interval in the study area **(Figure 10).**

Results

Interactive Classification

The rectangular frame separating the dark gray circle from the light gray circle in **Figure 7b** is called a discriminator. Note that many of the measurements cannot be separated in **Figure 7a**. Because Gong and Zhao, (2009) found that increased brittleness improved TBM performance, we examine brittleness as a means to predict COP. Altamar and Marfurt (2014) used geomechanical properties to predict brittleness index for shale plays in the USA. We display a crossplot in **Figure 9** where each sample was color-coded bzy COP and plotted in a 2D space. Then we manually defined high COP (red), low COP (green) and mixed COP (yellow) polygons to define a 3-cluster template. A crossplot of $\lambda\rho$ and $\mu\rho$ in **Figure 9a** illustrates the limitations of manually picking clusters in two-attribute space, where 50% of the voxels fall into the mixed COP (yellow) class. **Figure 9b**, a crossplot of ρ and V_p/V_s, further shows this problem with the handpicked clusters where an even larger number of voxels falls into the mixed (yellow) class.

Figure 8 suggests improved class separation when using three attributes. However, drawing a template is significantly more challenging than in **Figure 6**.

PSVM Classification

Visualization and interactive visualization with more than three attributes is intractable. *PSVM* addresses this problem in two ways. First, it projects the data, in this case, two attributes defining a 2D space that cannot be separated by a linear discriminator, into a higher *3*-dimensional space (**Figure 7**) where separation by a planar discriminator is possible. Second, because the discriminator generation is machine driven rather than interpreter driven, one can introduce more than three input attributes. We used the five attributes, curvedness, $\lambda\rho$, $\mu\rho$, porosity, and P-impedance which found to exhibit good histogram separation in all exploratory data analysis steps (**Figure 3**). The PSVM method allows us to create a classification model based on a set of training input. As the dimensionality of the input increases, the model becomes more accurate at classifying COP within the dataset. For instance, during the validation process, we found the model to be sensitive to porosity. Before porosity was introduced to the model, the accuracy was 88.9%. When porosity was added as a new degree of dimensionality, the accuracy increased to 94%. This allowed for the creation of an optimal model with five degrees of dimensionality for COP classification across the study area.

A comparison of the histograms (**Figure 4**) shows that the generated PSVM model is more sensitive to geomechanical rock properties than geometric attributes. Indeed, strain (measured by curvature) is only one component necessary to generate natural fractures. Stearns (2015) found fractures measured in horizontal image logs were highly correlated to gamma ray (lithology) response and only less connected to curvature, if at all. Nevertheless, this is not to say structural attributes such as curvature have no effect on the model. We observed that higher COP values are linked with higher curvedness, which indicated that it is harder to drill through the formation with higher structural complexities. Studies have found that large curvature values are related with natural fractures, which may or not be cemented (Bourgoyne et al., 1986; Hunt et al., 2011). Such heterogeneities may slow the drilling progress. Porosity is another a good indicator of microstructures associated with fracture geometry. Low porosity observed in low COP wells may seem counter-intuitive at first; however, woodworkers observe that there are few bit problems when drilling through oak, but that the bit often gets stuck or even breaks when drilling relatively “soft” pine (Neher, 1993). Again using the woodworker’s analogy, one uses different saw blades for different woods. The bits used in this survey may have been chosen to deal effectively with the very hard chert.

Conclusions

COP is a major factor affecting the time spent drilling a well and is directly related to the overall cost of the drilling process. This is the first study that links COP to seismic data and seismic-related attributes. Clustering five attributes using a PSVM classification method, we were able to correlate COP with seismic attributes and geomechanical rock properties and obtain a confidence of 94%. Low COP was observed in wells encountering low porosity, high $\lambda\rho$, high $\mu\rho$, low curvedness and high P-impedance. High COP was observed in wells encountering high porosity, low $\lambda\rho$, low $\mu\rho$, high curvedness and low P-impedance. By using this workflow, we can use COP of previously drilled wells with 3D seismic data to predict COP over the study area. While one may still wish to drill a specific target objective, we claim that this statistical analysis technique will provide a more accurate cost estimate and help choose the appropriate drilling equipment.

References

Altamar, R. P., and K. Marfurt, 2014, Mineralogy-based brittleness prediction from surface seismic data: Application to the Barnett Shale: Interpretation, v. 2, no. 4, p. T255–T271, doi:10.1190/INT-2013-0161.1.

Bass, N. W., 1942, Subsurface geology and oil and gas resources of Osage County, Oklahoma, in U. S. Geological Survey Bulletin 900-K: p. 343–393.

Bourgoyne, A. T., K. K. Millheim, M. E. Chenevert, and F. S. Young Jr, 1986, Applied Drilling Engineering Chapter **8** Solutions. Society of Petroleum Engineers.

Costello, D., M. Dubois, and R. Dayton, 2013, Core to characterization and modeling of the Mississippian, North Alva area, Woods and Alfalfa Counties, Oklahoma, *in* 2013 Mid-Continent Section AAPG Core Workshop: from source to reservoir to seal: Wichita, KS, p. 165–175.

Dowdell, B. L., J. T. Kwiatkowski, and K. J. Marfurt, 2013, Seismic characterization of a Mississippi Lime resource play in Osage County, Oklahoma, USA: Interpretation, v. 1, no. 2, p. SB97–SB108, doi:10.1190/INT-2013-0026.1.

Farrokh, E., J. Rostami, and C. Laughton, 2012, Study of various models for estimation of penetration rate of hard rock TBMs: Tunnelling and Underground Space Technology, v. 30, p. 110–123, doi:http://dx.doi.org/10.1016/j.tust.2012.02.012.

Gong, Q. M., and J. Zhao, 2009, Development of a rock mass characteristics model for TBM penetration rate prediction: International Journal of Rock Mechanics and Mining Sciences, v. 46, no. 1, p. 8–18, doi:http://dx.doi.org/10.1016/j.ijrmms.2008.03.003.

Gong, Q. M., J. Zhao, and Y. S. Jiang, 2007, In situ TBM penetration tests and rock mass boreability analysis in hard rock tunnels: Tunnelling and Underground Space Technology, v. 22, no. 3, p. 303–316, doi:http://dx.doi.org/10.1016/j.tust.2006.07.003.Harris, N. B., J. L. Miskimins, and C. A. Mnich, 2011, Mechanical anisotropy in the Woodford Shale, Permian Basin: Origin, magnitude, and scale: The Leading Edge, v. 30, no. 3, p. 284–291, doi:10.1190/1.3567259.

Hunt, L., S. Reynolds, S. Hadley, J. Downton, and S. Chopra, 2011, Causal fracture prediction: Curvature, stress, and geomechanics: The Leading Edge, v. 30, no. 11, p. 1274–1286, doi:10.1190/1.3663400.

King, C. H., and M. D. Pinckard, 2000, Method of and system for optimizing rate of penetration in drilling operations, US6026912A: Google Patents.

Lindzey, K., M. J. Pranter, and K. Marfurt, 2015, Geologically Constrained Seismic Characterization and 3-D Reservoir Modeling of Mississippian Reservoirs, North Central Anadarko Shelf, Oklahoma, *in* AAPG Annual Convention and Exhibition, Tulsa, OK, USA.

Mazzullo, S. J., B. W. Wilhite, and I. W. Woolsey, 2009, Petroleum reservoirs within a spiculite-dominated depositional sequence: Cowley Formation (Mississippian: Lower Carboniferous), south-central Kansas: AAPG bulletin, v. 93, no. 12, p. 1649–1689.

Montgomery, S. L., J. C. Mullarkey, M. W. Longman, W. M. Colleary, and J. P. Rogers, 1998 Mississippian “Chat” Reservoirs, South Kansas: Low-Resistivity Pay in a Complex Chert Reservoir: AAPG Bulletin, v. 82, p. 187-205.

Neher, H. V., 1993, Effects of pressures inside Monterey pine trees: Trees, v. 8, no. 1, p. 9–17, doi:10.1007/BF00240976.

Parham, K. D., and R. A. Northcutt., 1993, Mississippian chert and carbonate basal Pennsylvanian sandstone; Central Kansas Uplift and northern Oklahoma, *in* Atlas of major midcontinent gas reservoirs: Texas Bureau of Economic Geology, Austin, TX, Gas Research Institute.

Perez, R., and K. Marfurt, 2013, Brittleness estimation from seismic measurements in unconventional reservoirs: Application to the Barnett Shale, *in* 2013 SEG Annual Meeting, Houston, TX, USA.

Rogers, S. M., 2001, Deposition and diagenesis of Mississippian chat reservoirs, North-Central Oklahoma: AAPG Bulletin, v. 85, no. 1, p. 115–129, doi:10.1306/8626C771-173B-11D7-8645000102C1865D.

Roy, A., B. L. Dowdell, and K. J. Marfurt, 2013, Characterizing a Mississippian tripolitic chert reservoir using 3D unsupervised and supervised multiattribute seismic facies analysis: An example from Osage County, Oklahoma: Interpretation, v. 1, no. 2, p. SB109–SB124, doi:10.1190/INT-2013-0023.1.

Da Silva, M., and K. Marfurt, 2012, Framework for EUR correlation to Seismic Attributes in the Barnett Shale, TX, *in* 2012 SEG Annual Meeting, Las Vegas, NV, USA.

Stearns, V. T., 2015, Fracture characterization of the Mississippi lime utilizing whole core, horizontal borehole images, and 3D seismic data from a mature field in Noble County Oklahoma: MS thesis University of Oklahoma.

Verma, S., O. Mutlu, and K. J. Marfurt, 2013, Seismic modeling evaluation of fault illumination in the Woodford Shale, *in* 2013 SEG Annual Meeting, Houston, Texas USA.

Verma, S., T. Zhao, K. J. Marfurt, and D. Devegowda, 2016, Estimation of total organic carbon and brittleness volume: Interpretation, v. 4, no. 3, p. T373–T385, doi:10.1190/INT-2015-0166.1.

Watney, W. L., W. J. Guy, and A. P. Byrnes, 2001, Characterization of the Mississippian chat in south-central Kansas: AAPG bulletin, v. 85, no. 1, p. 85–113.

White, H., B. Dowdell, and K. J. Marfurt, 2012, Calibration of surface seismic attributes to natural fractures using horizontal image logs, Mississippian Lime, Osage County, Oklahoma, *in* 2012 SEG Annual Meeting, Las Vegas, NV, USA.

Zhang, B., T. Zhao, X. Jin, and K. Marfurt, 2015, Brittleness evaluation of resource plays by integrating petrophysical and seismic data analysis: Interpretation, v. 3, no. 2, p. T81–T92, doi:10.1190/INT-2014-0144.1.

Zhao, T., V. Jayaram, K. J. Marfurt, and H. Zhou, 2014, Lithofacies classification in Barnett Shale using Proximal Support Vector Machines, *in* 2014 SEG Annual Meeting, Denver, CO, USA.

Zhao, T., V. Jayaram, A. Roy, and K. J. Marfurt, 2015, A comparison of classification techniques for seismic facies recognition: Interpretation, v. 3, no. 4, p. SAE29–SAE58, doi:10.1190/INT-2015-0044.1.

Figure captions

Figure 1. (a) Major geologic provinces of Oklahoma with the area of interest outlined in red. (Modified from Johnson and Luza (2008); Northcutt and Campbell (1996)). (b) a type log showing the Mississippian Limestone section in the area of interest (Modified from Lindzey et al., 2015).

Figure 2. (a) Workflow for attribute generation and depth conversion, (b) data analysis of the extracted parameters, (c) the training process, and (d) the validation process.

Figure 3. The mean and standard deviation of COP for 51 horizontal wells that fall within the 3D seismic survey. We separate these wells into two classes: seven high COP (the grey cluster) and forty-four low COP wells (the white cluster). The dashed line is called the discriminator between the two clusters.

Figure 4. Exploratory data analysis using the work flow shown in Figure 2b. Showing five attributes exhibiting good histogram separation between high COP (in dark gray) and low COP (in light gray) along all well trajectories: (a) curvedness, (b) $\lambda\rho$, (c) $\mu\rho$, (d) P-impedance, and (e) porosity. (f) Results of the validation test using seven low and seven high COP wells which are highlighted by gray circle in Figure 3. With increases in the number of inputs (from one to five), the accuracy increases accordingly.

Figure 5. Horizon probes along the top of Mississippian Limestone through (a) porosity, (b) $\lambda\rho$, (c) $\mu\rho$, and (d) P-impedance volumes. Red and green well paths denote representative high and low COP wells, respectively.

Figure 6. Co-rendered the most positive (k_1) and the most negative (k_2) curvature along the top of the picked Mississippian horizon with two representative high and low COP wells paths. The opacity curve is applied to k_1 and k_2.

Figure 7. (a) when two different clusters are impossible to separate by a line in a 2-D space. (b) increasing the dimensionality to 3 through a nonlinear attribute transformation allows separation of the two classes by a plan.

Figure 8. (a) Similarly, high and low COP is difficult to discriminate when using $\lambda\rho$ and curvedness in a 2-D space. (b) Discrimination becomes easier by adding a third porosity axis.

Figure 9. (a) An interactive classification in $\lambda\rho$-$\mu\rho$ space. Along the wellbore we have $\lambda\rho$, $\mu\rho$ and COP triplets. Each sample is color-coded along the well by its COP and plot in $\lambda\rho$-$\mu\rho$ space. Red, green and mixed cluster polygons are hand-drawn polygons around each cluster. This template is then used to color-code voxels between the top of the Mississippian Limestone and the top of Woodford. Red and green well paths denote representative high and low COP wells. In (b) Classification in ρ-V_p/V_s space. Triplets of ρ, V_p/V_s and COP are sampled along the wellbore, crossplotted, and a new template constructed and used to color code the Mississippian interval. Note that neither template accurately predicts the COP of these two wells.

Figure 10. Horizon probe of COP on the Mississippian Limestone computed using the five attributes shows in Figure 4-6 and a PSVM classifier. Note that the two representative wells now fall along voxels corresponding to their observed COP value.

a)

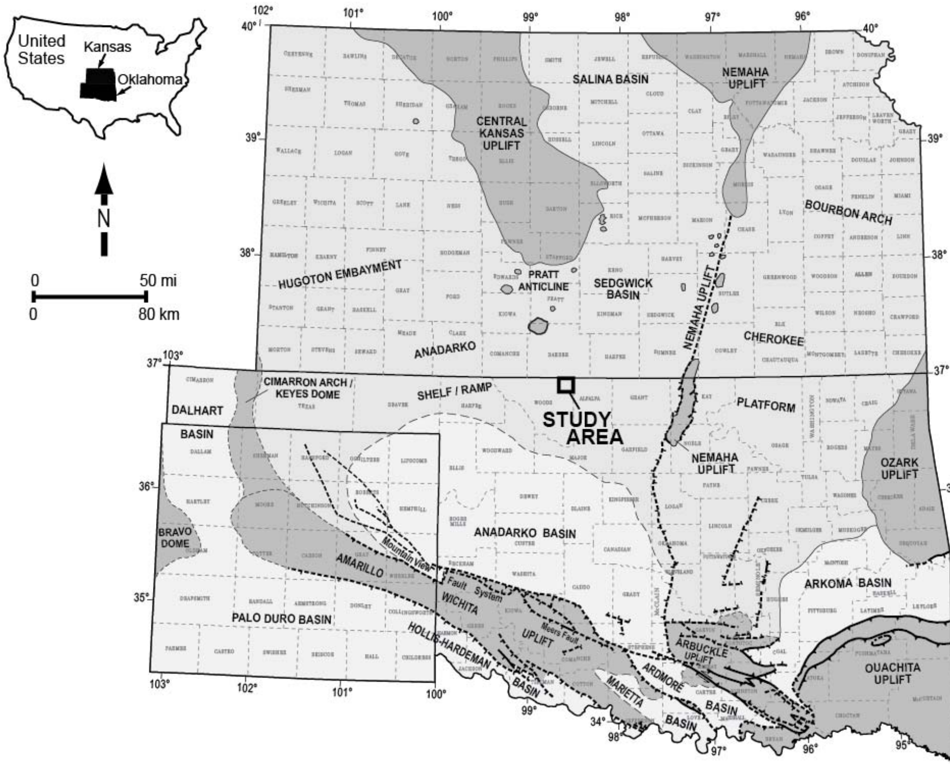
United States
Kansas
Oklahoma
N
0 50 mi
0 80 km
102°
101°
100°
99°
98°
97°
96°
40°
39°
38°
37°
36°
35°
34°
103°
95°
SALINA BASIN
NEMAHA UPLIFT
CENTRAL KANSAS UPLIFT
BOURBON ARCH
HUGOTON EMBAYMENT
PRATT ANTICLINE
SEDGWICK BASIN
NEMAHA UPLIFT
CHEROKEE
ANADARKO
SHELF / RAMP
CIMARRON ARCH / KEYES DOME
DALHART BASIN
STUDY AREA
PLATFORM
NEMAHA UPLIFT
OZARK UPLIFT
BRAVO DOME
ANADARKO BASIN
Mountain View Fault System
AMARILLO
WICHITA
UPLIFT
Meers Fault
ARKOMA BASIN
PALO DURO BASIN
HOLLIS-HARDEMAN BASIN
ARBUCKLE UPLIFT
ARDMORE BASIN
MARIETTA BASIN
OUACHITA UPLIFT

b)

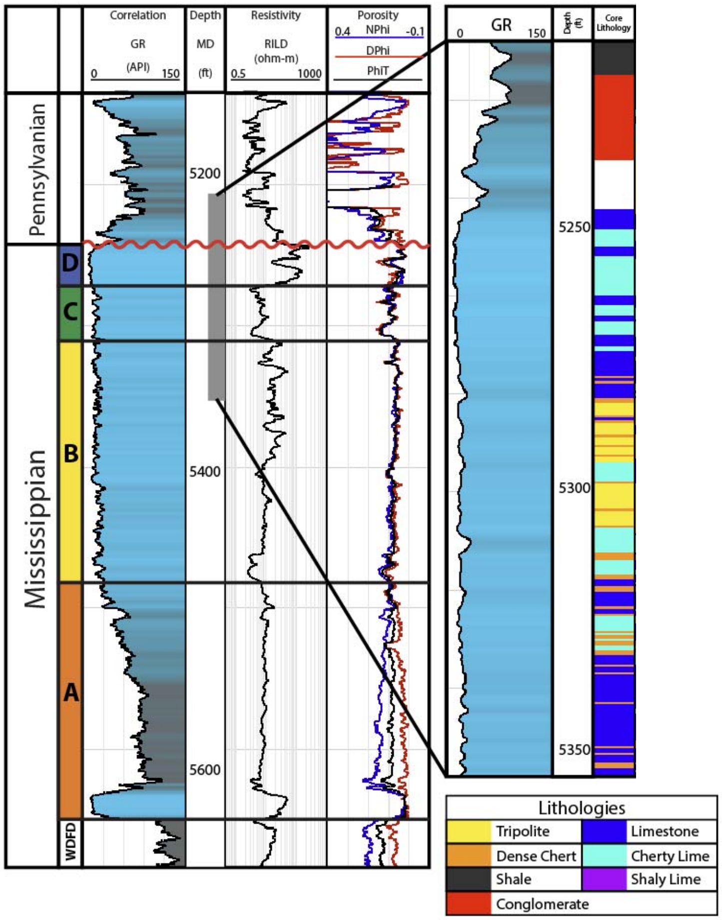

Figure 1. (a) Major geologic provinces of Oklahoma with the area of interest outlined in red. (Modified from Johnson and Luza (2008); Northcutt and Campbell (1996)). (b) a type log showing the Mississippian Limestone section in the area of interest (Modified from Lindzey et al., 2015).

a)

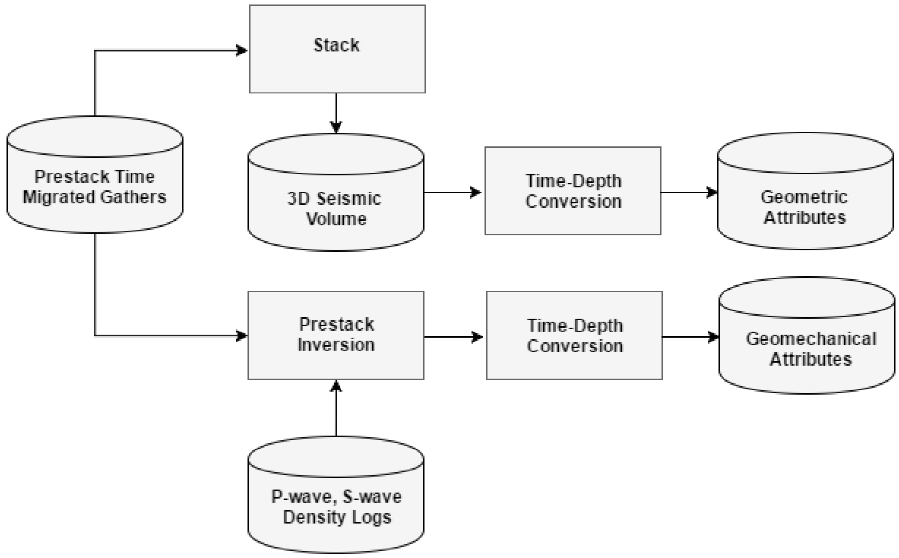
Stack
Prestack Time Migrated Gathers
3D Seismic Volume
Time-Depth Conversion
Geometric Attributes
Prestack Inversion
Time-Depth Conversion
Geomechanical Attributes
P-wave, S-wave Density Logs

b)

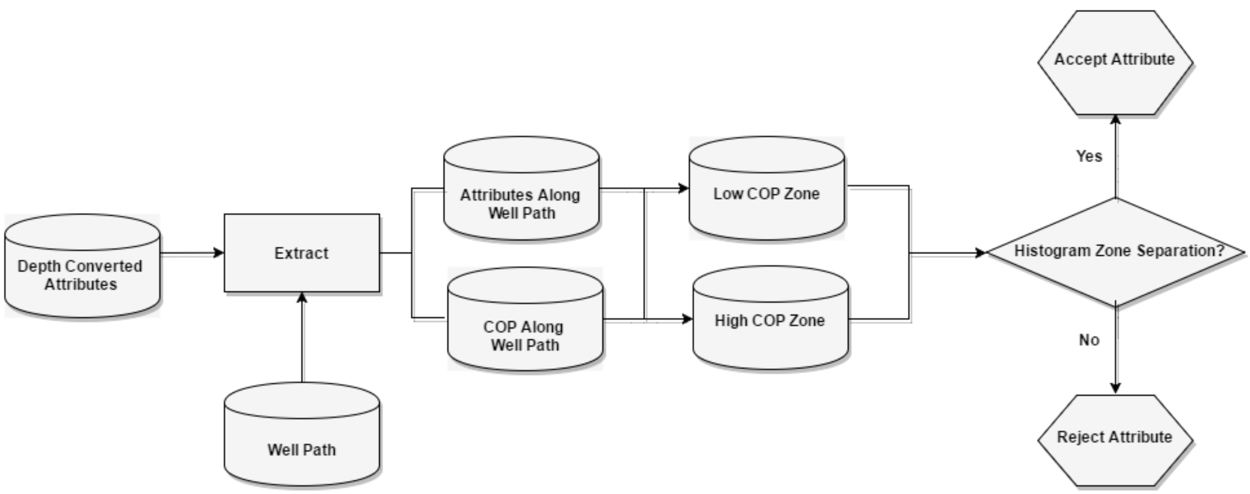
Accept Attribute
Yes
Attributes Along Well Path
Low COP Zone
Depth Converted Attributes
Extract
Histogram Zone Separation?
COP Along Well Path
High COP Zone
No
Well Path
Reject Attribute

c)

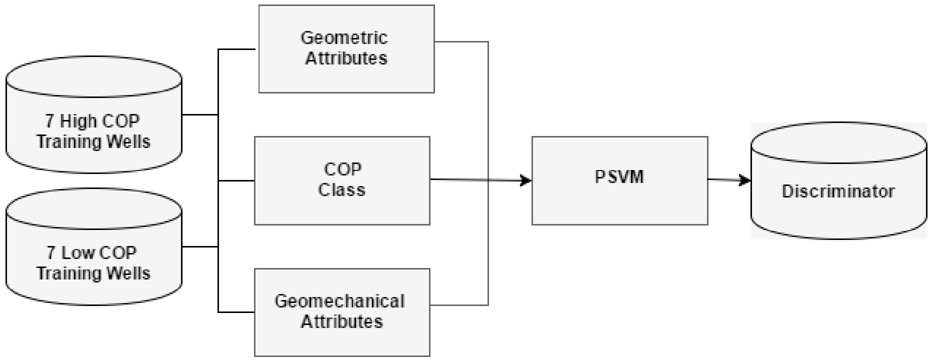

d)

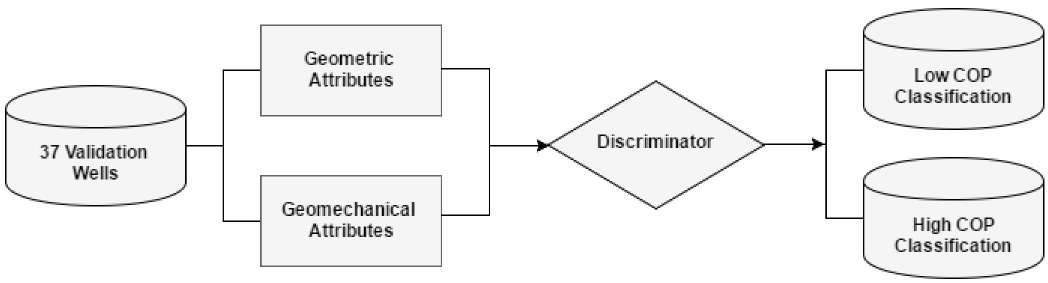

Figure 2. (a) Workflow for attribute generation and depth conversion, (b) data analysis of the extracted parameters, (c) the training process, and (d) the validation process.

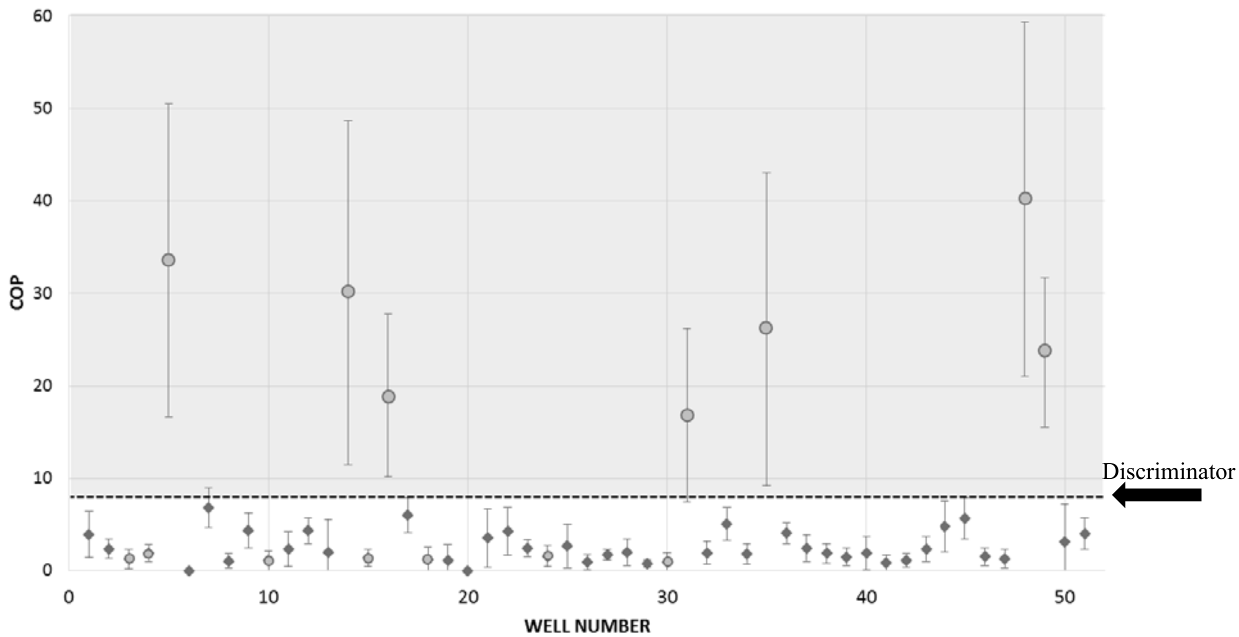

Figure 3. The mean and standard deviation of COP for 51 horizontal wells that fall within the 3D seismic survey. We separate these wells into two classes: seven high COP (the grey cluster) and forty-four low COP wells (the white cluster). The dashed line is called the discriminator between the two clusters.

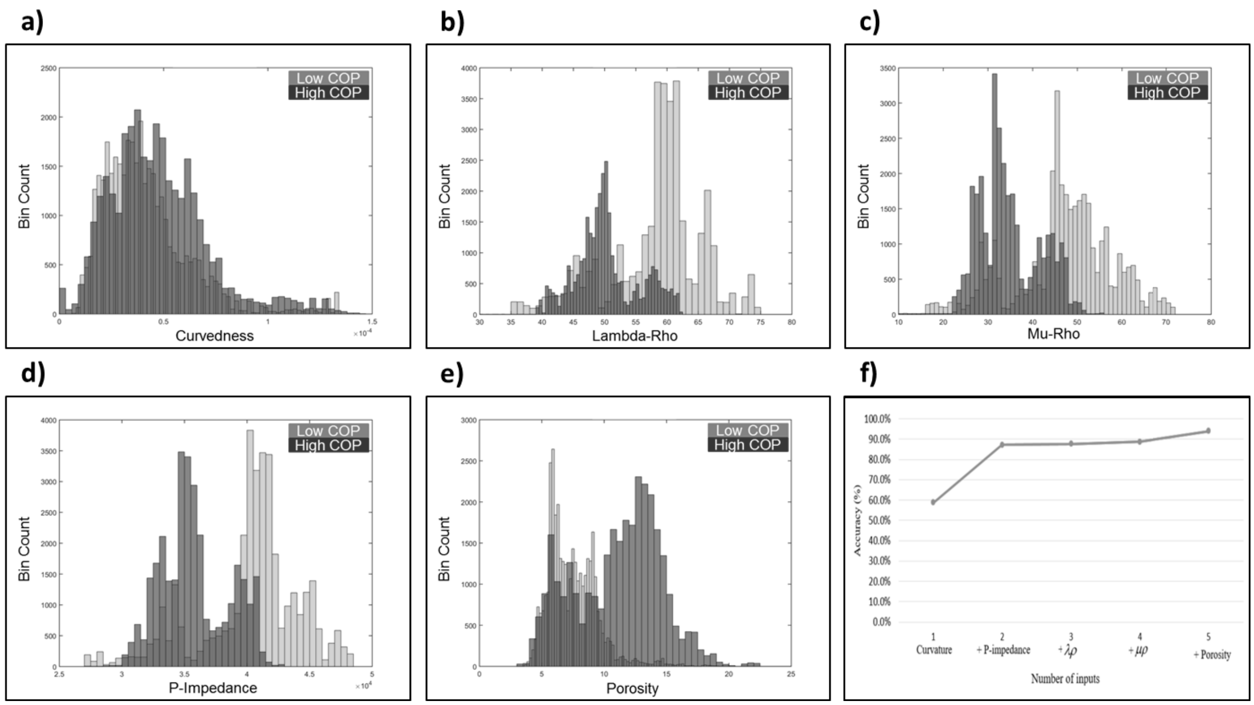

Figure 4. Exploratory data analysis using the work flow shown in Figure 2b. Showing five attributes exhibiting good histogram separation between high COP (in dark gray) and low COP (in light gray) along all well trajectories: (a) curvedness, (b) $\lambda\rho$, (c) $\mu\rho$, (d) P-impedance, and (e) porosity. (f) Results of the validation test using seven low and seven high COP wells which are highlighted by gray circle in Figure 3. With increases in the number of inputs (from one to five), the accuracy increases accordingly.

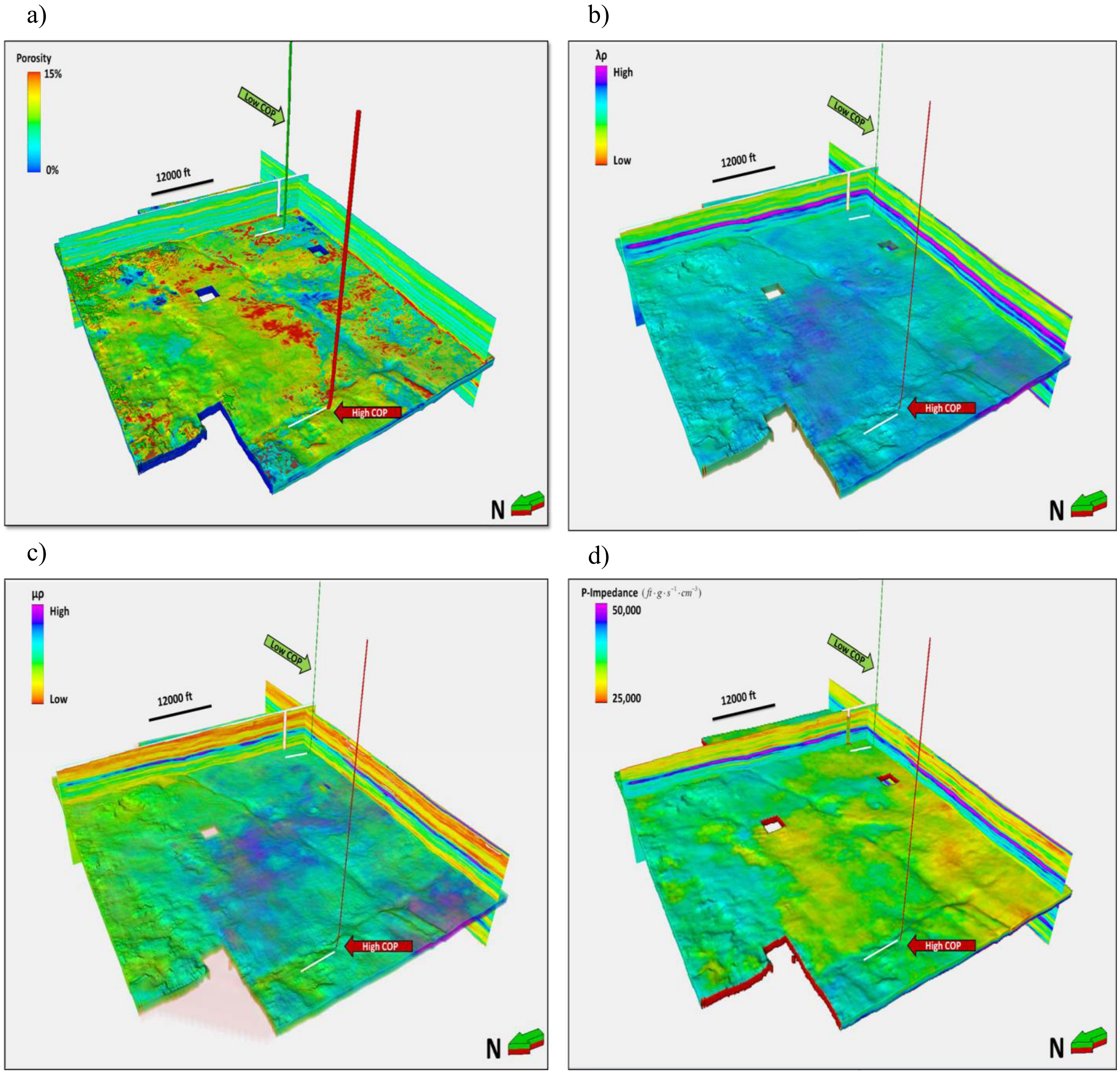

Figure 5. Horizon probes along the top of Mississippian Limestone through (a) porosity, (b) $\lambda\rho$, (c) $\mu\rho$, and (d) P-impedance volumes. Red and green well paths denote representative high and low COP wells, respectively.

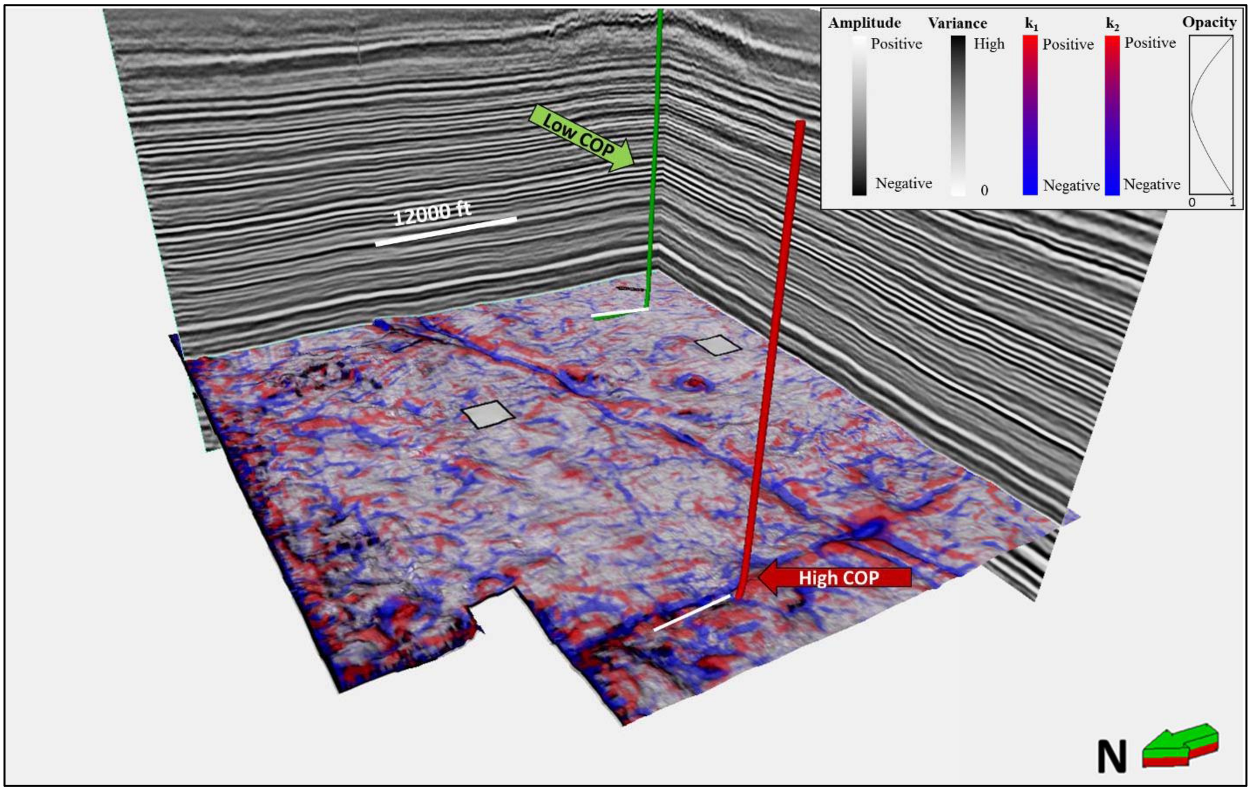

Figure 6. Co-rendered the most positive (k_1) and the most negative (k_2) curvature along the top of the picked Mississippian horizon with two representative high and low COP wells paths. The opacity curve is applied to k_1 and k_2.

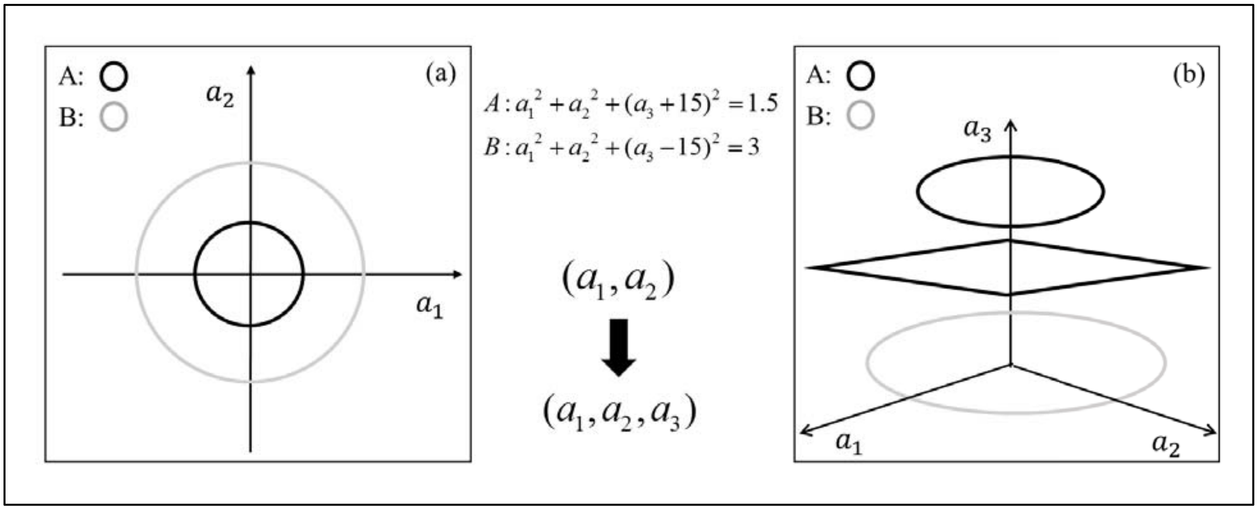

Figure 7. (a) when two different clusters are impossible to separate by a line in a 2-D space. (b) increasing the dimensionality to 3 through a nonlinear attribute transformation allows separation of the two classes by a plan.

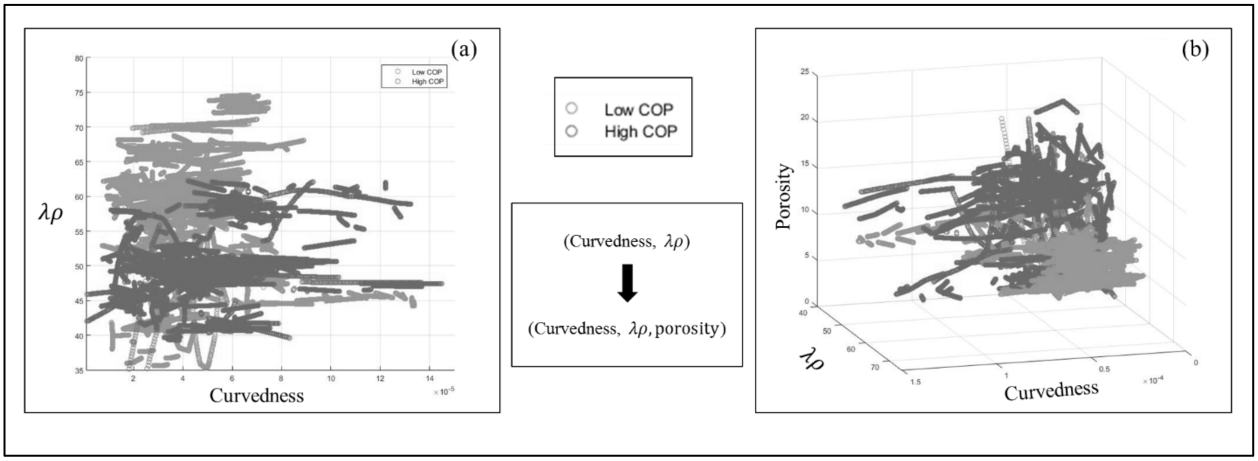

Figure 8. (a) Similarly, high and low COP is difficult to discriminate when using $\lambda\rho$ and curvedness in a 2-D space. (b) Discrimination becomes easier by adding a third porosity axis.

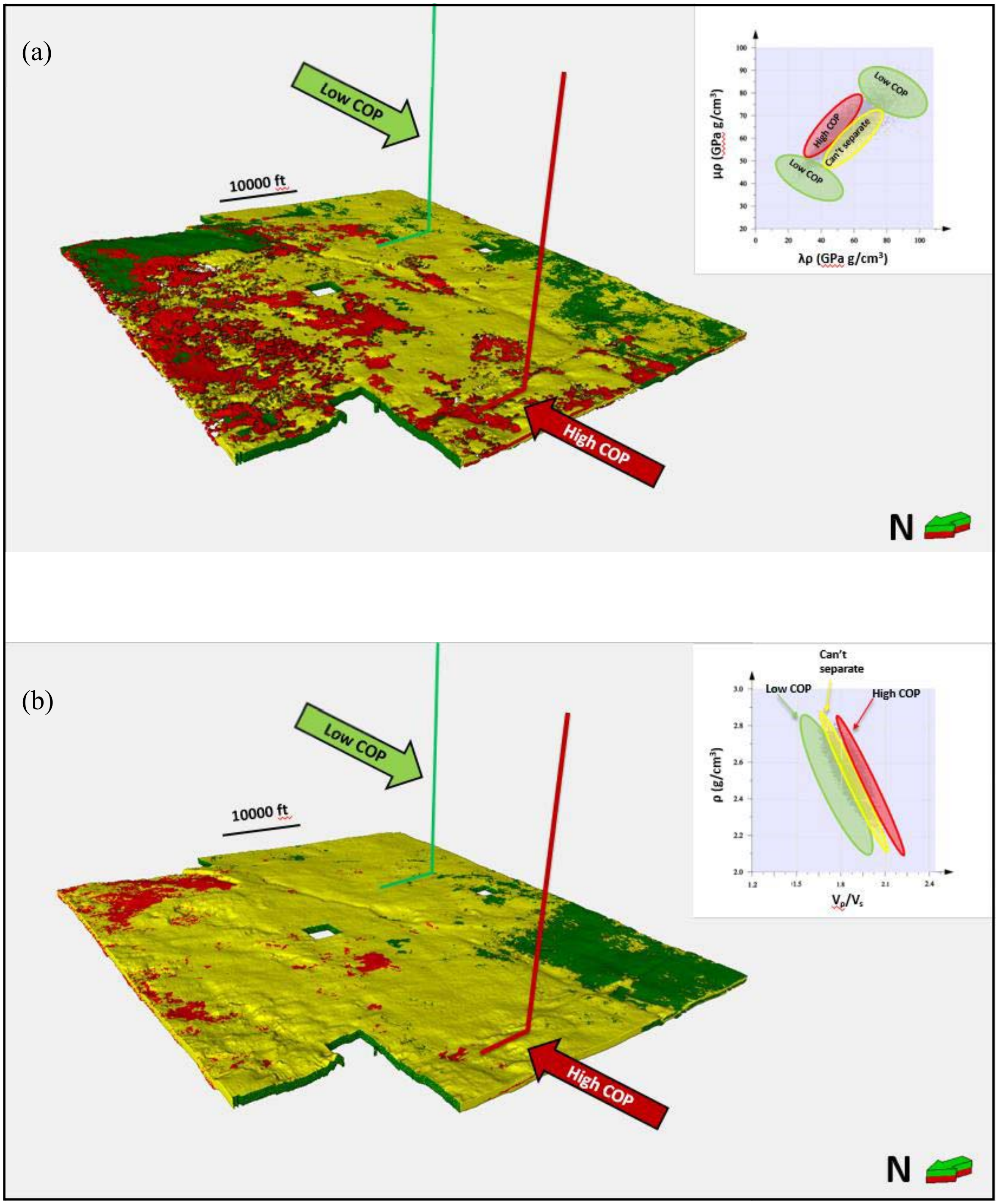

Figure 9. (a) An interactive classification in λρ-μρ space. Along the wellbore we have λρ, μρ and COP triplets. Each sample is color-coded along the well by its COP and plot in λρ-μρ space. Red, green and mixed cluster polygons are hand-drawn polygons around each cluster. This template is then used to color-code voxels between the top of the Mississippian Limestone and the top of Woodford. Red and green well paths denote representative high and low COP wells. In (b) Classification in ρ-V_p/V_s space. Triplets of ρ, V_p/V_s and COP are sampled along the wellbore, crossplotted, and a new template constructed and used to color code the Mississippian interval. Note that neither template accurately predicts the COP of these two wells.

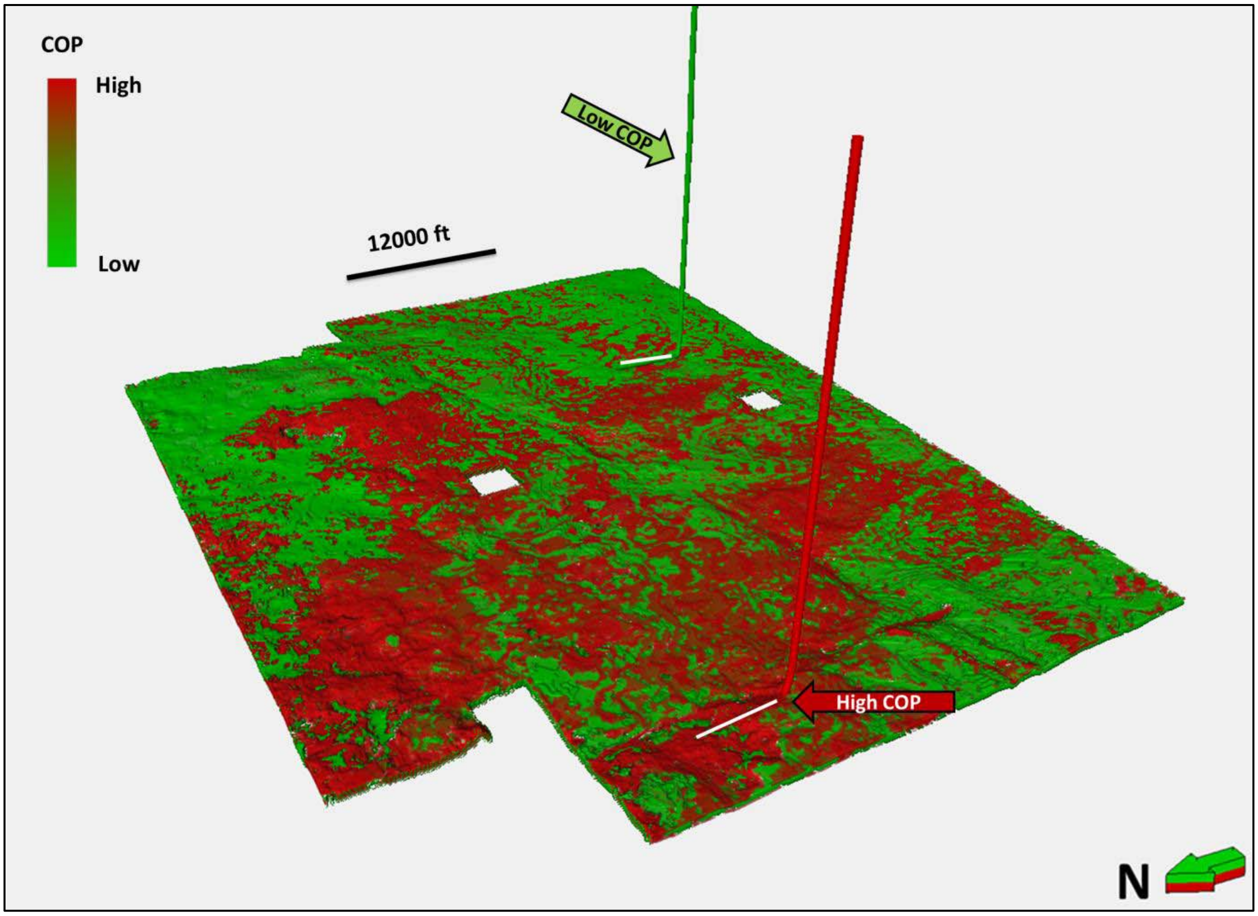

Figure 10. Horizon probe of COP on the Mississippian Limestone computed using the five attributes shows in Figure 4-6 and a PSVM classifier. Note that the two representative wells now fall along voxels corresponding to their observed COP value.